



# Fabrication of high performance Pt/Ti counter electrodes on Ti mesh for flexible large-area dye-sensitized solar cells

Yaoming Xiao, Jihuai Wu\*, Gentian Yue, Jianming Lin, Miaoliang Huang, Leqing Fan, Zhang Lan

Engineering Research Center of Environment-Friendly Functional Materials, Ministry of Education, Institute of Materials Physical Chemistry, Huaqiao University, Quanzhou 362021, China

## ARTICLE INFO

### Article history:

Received 29 August 2011  
Received in revised form 2 October 2011  
Accepted 2 October 2011  
Available online 8 October 2011

### Keywords:

Pt counter electrode  
Ti mesh  
Large area  
Flexible dye-sensitized solar cell

## ABSTRACT

High performance and homogeneous platinum (Pt) nanoparticles is electrodeposited onto titanium (Ti) mesh to form counter electrodes for use in large-area flexible dye-sensitized solar cells (DSSCs). The obtained Pt/Ti counter electrode shows high electrocatalytic activity for the  $I_3^-/I^-$  redox reaction, low charge transfer resistance ( $49.57 \Omega \text{ cm}^2$  with an area of  $80 \text{ cm}^2$ ) and good light transmittance (92.31%). Based on the counter electrode, a light-to-electric energy conversion efficiency of 6.13% is achieved for a flexible DSSC with an area of  $80 \text{ cm}^2$ , and a maximum power output of 0.443 W is reached for a flexible DSSC with an area of  $160 \text{ cm}^2$ , under an outdoors natural light irradiation with an intensity of  $55 \text{ mW cm}^{-2}$ . The present findings should accelerate the practical application of flexible DSSCs.

© 2011 Elsevier Ltd. All rights reserved.

## 1. Introduction

Since the first dye-sensitized solar cell (DSSC) was reported in 1991 by O' Regan and Grätzel, substantial research has been conducted in this area, resulting in the production of a DSSC with a photoelectric conversion efficiency that is as high as 12% [1–3]. DSSCs and polymer solar cells [4–7] are considered the third generation of photovoltaic cells to use roll-to-roll processing, which could be a promising solution for many impending energy and environmental problems. A typical DSSC consists of a dye-sensitized porous nanocrystalline  $\text{TiO}_2$  film electrode, a redox electrolyte and a platinized counter electrode. The function of the counter electrode is to transfer electrons from the external circuit back to the redox electrolyte to catalyze the reduction of the triiodide ion [8,9]. To meet the demand for renewable energy and industrialization, flexible DSSCs have attracted wide interest because of their many advantageous properties, including a light weight, good flexibility, impact-proof properties and low cost. The flexible DSSC's shape or surface can be purposefully designed, and large-scale continuous production and rapid coating can be used to fabricate these devices, further decreasing their cost [10–13]. Pt counter electrodes on flexible substrates are usually prepared by sputtering, electrochemical deposition, or chemical reduction. Ikegami et al. deposited a Pt/Ti

bilayer on ITO-PEN substrates using vacuum sputtering and assembled a full plastic DSSC, achieving a conversion efficiency of 4.31% [14]. Grätzel and co-workers electrodeposited a Pt catalyst on an ITO/PEN substrate to assemble a flexible DSSC with a conversion efficiency of 7.2% [15]. Thomas et al. electrodeposited Pt on single-walled carbon nanotube networks [16]. Kang et al. [17] and Park et al. [18] used chemical reduction to prepare Pt counter electrodes by coating conductive plastic substrates with an  $\text{H}_2\text{PtCl}_6 \cdot 6\text{H}_2\text{O}$  2-propanol solution and then reducing  $\text{Pt}^{4+}$  in a  $\text{NaBH}_4$  solution.

Reports concerning large DSSCs have previously been published [19–25]. A high electrocatalytic activity for the  $I_3^-/I^-$  redox reaction and the low charge transfer resistance of the substrate is very significant in improving the performance of DSSCs, especially from the perspectives of large-scale production [22,23,25]. Metal foils, such as stainless steel and titanium foil, have been utilized as anode electrodes to manufacture flexible DSSCs because of their flexibility and relatively low sheet resistance compared with conducting glass substrates [11,12,15,17,18]. In addition, the conducting grid has been considered as a carrier collector for the large-area DSSC to improve the electrical interconnections of the cells. Ag foil has been actively investigated because of its low sheet resistance, low dark current and low cost [22,25]. However, the unacceptably high corrosion (or dissolution) of Ag in the contacting  $I^-/I_3^-$  electrolyte has been a critical issue to overcome [23].

Ti foils and Ti mesh have relatively low sheet resistances and superior corrosion resistances in the contacting  $I^-/I_3^-$  electrolyte because of the passive oxide film of  $\text{TiO}_2$  on these substrates. In this

\* Corresponding author. Tel.: +86 595 22693899; fax: +86 595 22692229.  
E-mail address: [jhwu@hqu.edu.cn](mailto:jhwu@hqu.edu.cn) (J. Wu).

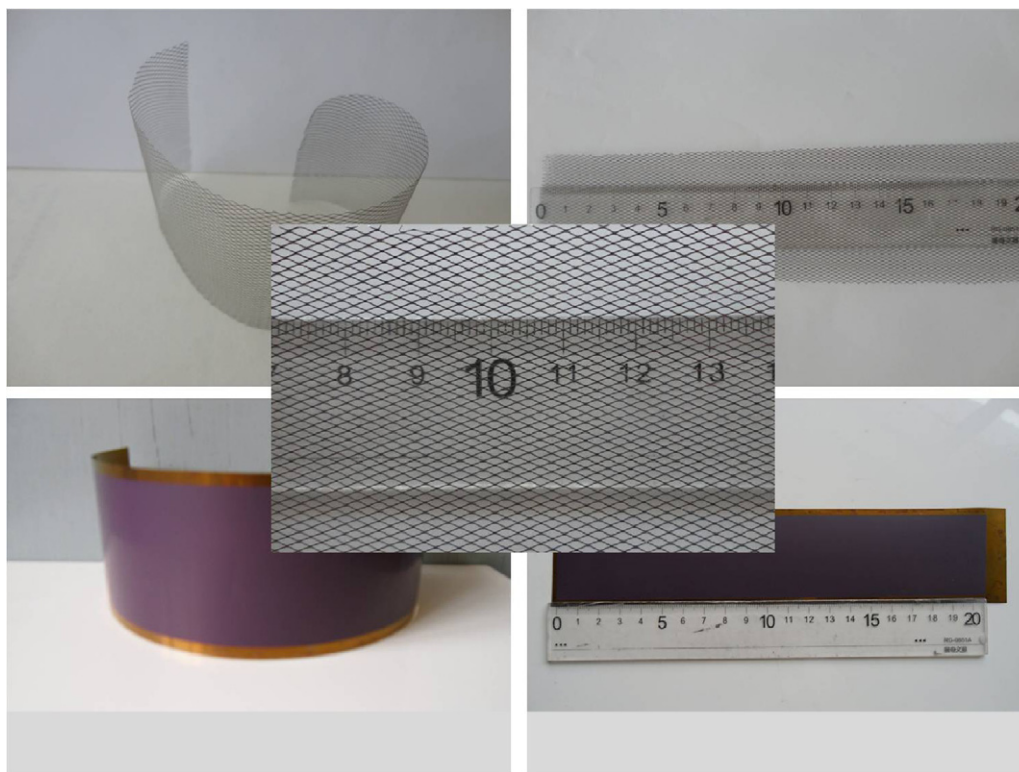


Fig. 1. Photographs of the large-area flexible TiO<sub>2</sub>/Ti anode and Pt/Ti counter electrode.

paper, we report the fabrication and characterization of large-area, flexible, dye-sensitized solar cells based on TiO<sub>2</sub> anode electrode on a Ti foil and Pt/Ti counter electrode on a Ti mesh (see Fig. 1).

## 2. Experimental

### 2.1. Materials

H<sub>2</sub>PtCl<sub>6</sub>·6H<sub>2</sub>O, ethanol, iodine, lithium iodide, tetrabutyl ammonium iodide, 4-tert-butyl-pyridine (TBP), acetonitrile (AN), tetrabutyl titanate, titanium tetrachloride, hydrofluoric acid, hydrochloric acid, nitric acid, PEG-20000 and Triton X-100 were purchased from the Shanghai Chemical Agent Ltd., China (Analytical grade purity). Sensitized-dye N719 [cis-di(thiocyanato)-N,N'-bis (2,2'-bipyridyl-4-carboxylic acid-4-tetrabutylammonium carboxylate) ruthenium (II)] was purchased from Solaronix SA, Switzerland. The above reagents were used without further purification.

### 2.2. Fabrication of flexible Pt/Ti counter electrodes

Pt/Ti counter electrodes on Ti mesh were electrodeposited by using the current–time (chronoamperometry) technique from an aqueous solution containing 2.0 mM H<sub>2</sub>PtCl<sub>6</sub> in a 0.50 M HCl aqueous solution. A three-electrode cell with an Electrochemical Workstation (CHI660D, Shanghai Chenhua Device Company, China) consisting of the Ti mesh (0.05 mm thickness, purchased from Anheng Wire Mesh Co., Ltd., China) working electrode, a Pt wire counter electrode and an Ag/AgCl reference electrode was used in these studies. Before plating, Ti mesh samples with rectangular dimensions of 21 cm × 4.5 cm, 21 cm × 6.5 cm and 21 cm × 8.5 cm were cleaned with mild detergent and rinsed in distilled water. The mesh samples were then immersed in hydrofluoric acid solution at a suitable concentration for 2 min and rinsed again in distilled water. The current–time (chronoamperometry) plating of Pt thin films on the Ti mesh was carried out at an “Init E” of –0.35 V for

a “Run time” of 300 s (Fig. 2). The obtained Pt/Ti counter electrode was rinsed in distilled water and dried at 80 °C in a vacuum oven (Suzhou Jiangdong Precision Instrument Co., Ltd., China). For comparison, Pt/Ti counter electrodes carried out at an “Init E” of –0.35 V for “Run times” of 200 s and 400 s were also manufactured.

### 2.3. Preparation of flexible TiO<sub>2</sub>/Ti anode electrodes

Tetrabutyl titanate (20 mL) was rapidly added to distilled water (300 mL), leading to the immediate formation of a white precipitate. This precipitate was then filtered using a glass frit and washed three times with distilled water. The filter cake was added to a nitric acid solution (0.10 M, 200 mL) with vigorous stirring at 80 °C until the slurry became a translucent, homogeneous blue-white solution. The resulting colloidal suspension was autoclaved at 200 °C for 12 h

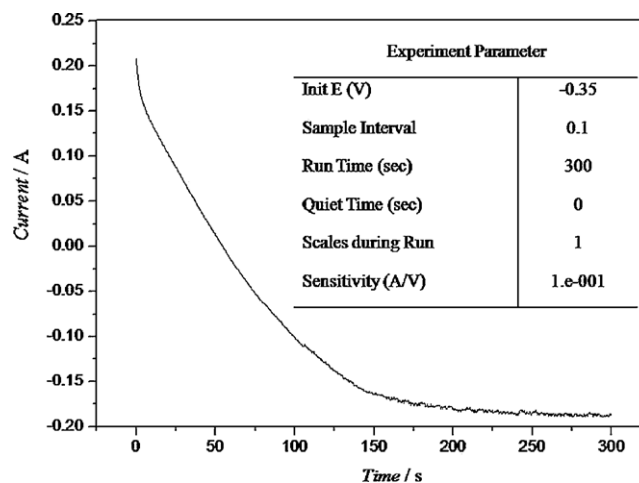


Fig. 2. Current–time for the electrodeposition of Pt on the Ti mesh.

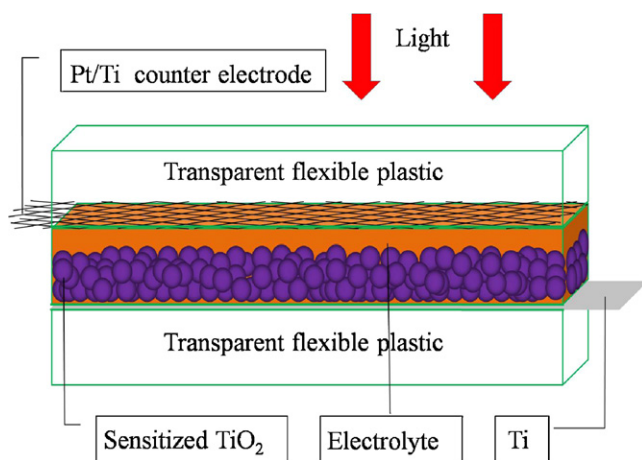


Fig. 3. Schematic diagram of large-area flexible dye-sensitized solar cells.

to form a milky white slurry. The resultant slurry was concentrated to one-quarter of its original volume, and then, PEG-20000 (10 wt% slurry) and a few drops of the Triton X-100 emulsification reagent were added to form a TiO<sub>2</sub> colloid. The TiO<sub>2</sub> colloid was coated on the titanium foil (0.03 mm thickness, purchased from Baoji Yunjie Metal Production Co., Ltd., China) using a doctor-scraping technique. Before the scraping, Ti foils with rectangular dimensions of 21 cm × 4.5 cm, 21 cm × 6.5 cm and 21 cm × 8.5 cm were washed with mild detergent and rinsed in distilled water. The foils were then immersed in a hydrofluoric acid solution of suitable concentration for 2 min and rinsed again in distilled water. The thickness of the TiO<sub>2</sub> film was controlled by the thickness of the adhesive tape around the edge of the cleaned Ti foil [26–28]. After drying at room temperature, the TiO<sub>2</sub> thin films were sintered at 450 °C for 30 min in air to produce nanocrystalline TiO<sub>2</sub> films. The TiO<sub>2</sub> electrodes were immersed in a 0.05 M TiCl<sub>4</sub> solution at 70 °C for 30 min and then washed three times with distilled water. The treated TiO<sub>2</sub> films were sintered at 400 °C for 20 min. When the TiO<sub>2</sub> electrodes were cooled to 80 °C, the obtained TiO<sub>2</sub>/Ti electrodes were treated with ultraviolet-O<sub>2</sub> at room temperature for 30 min. The TiO<sub>2</sub> flexible film was immersed in a 2.50 × 10<sup>-4</sup> M solution of dye N719 in absolute ethanol for 24 h, allowing sufficient time for the TiO<sub>2</sub> film to absorb the dye adequately to obtain a dye-sensitized TiO<sub>2</sub> flexible film electrode.

#### 2.4. Assemblage of flexible DSSC

The flexible DSSC was assembled by the injection of a redox-active electrolyte into the aperture between the TiO<sub>2</sub> film electrode (anode) and the Pt/Ti counter electrode (as shown in Fig. 3). The two electrodes were clipped together with two transparent flexible plastics, and a cyanoacrylate adhesive was used as a sealant to prevent the electrolyte solution from leaking. Epoxy resin was used to further seal the cell in order to enhance the cell stability. The redox electrolyte consisted of 0.60 M tetrabutyl ammonium iodide, 0.10 M lithium iodide, 0.10 M iodine and 0.50 M 4-tert-butyl-pyridine in acetonitrile.

#### 2.5. Characterization

The surface features of the flexible Pt/Ti counter electrode were observed using a scanning electron microscope (SEM, Hitachi S-4800, JAPAN) with an energy-dispersive X-ray spectrometer (EDS) attached. The cyclic voltammetry (CV) profiles of the Pt/Ti counter electrode were measured in a three-electrode electro-chemical cell with an Electrochemical Workstation (CHI660D, Shanghai Chenhua

Device Company, China) using the Pt/Ti as the working electrode, Pt-foil as the counter electrode, and an Ag/AgCl cell as a reference electrode, dipped in an acetonitrile solution of 10 mM LiI, 1 mM I<sub>2</sub>, and 0.1 M LiClO<sub>4</sub>. The CV measurements were performed using a CHI660D electrochemical measurement system (scan condition: 100 mV s<sup>-1</sup>). Electrochemical impedance spectroscopy (EIS) measurements of the large-area flexible DSSCs were carried out using a CHI660D electrochemical measurement system at a constant temperature of 20 °C with an AC signal amplitude of 20 mV in the frequency range from 0.1 to 10<sup>5</sup> Hz at 0 V DC bias in the dark.

#### 2.6. Photoelectrochemical measurements

The photovoltaic performance tests of the flexible DSSC were conducted by measuring the *I*-*V* character curves using a CHI660D electrochemical measurement system under irradiation with a natural light intensity (measured by Radiometer FZ-A, Photoelectric Inst. of Beijing Normal Univ., China) of 55 mW cm<sup>-2</sup> out of doors. The photovoltaic performance [i.e., fill factor (*FF*) and overall energy conversion efficiency (*η*)] of the DSSC were calculated using the following equations [29]:

$$FF = \frac{V_{\max} \times I_{\max}}{V_{OC} \times I_{SC}} \quad (1)$$

$$\eta (\%) = \frac{V_{\max} \times I_{\max}}{P_{in}} \times 100\% = \frac{FF \times V_{OC} \times I_{SC}}{P_{in}} \times 100\% \quad (2)$$

In these equations, *I*<sub>SC</sub> is the short-circuit current (A), *V*<sub>OC</sub> is the open-circuit voltage (V), *P*<sub>in</sub> is the incident light power (W), *I*<sub>max</sub> (A) and *V*<sub>max</sub> (V) are the current and voltage in the *I*-*V* curves, respectively, at the point of maximum power output.

### 3. Results and discussion

#### 3.1. Morphology and composition of Pt/Ti counter electrode

Fig. 4a shows the SEM image of the Pt/Ti counter electrode fabricated at an "Init E" of -0.35 V for a "Run time" of 300 s. It is obvious that a homogeneous Pt film has been electrodeposited on the Ti mesh with Pt nanoparticles approximately 20–30 nm in diameter. According to the EDS spectra (Fig. 4b), the Pt/Ti counter electrode consists of Pt and Ti, which indicates that the H<sub>2</sub>PtCl<sub>6</sub> was electrodeposited to form Pt using the chronoamperometry method.

#### 3.2. Electrodeposition times for the fabrication of Pt/Ti counter electrodes

Fig. 5a–c shows the SEM images of Pt/Ti counter electrodes that were electrodeposited for different times (200 s (Fig. 5a), 300 s (Fig. 5b) and 400 s (Fig. 5c)). It is obvious that the number of Pt nanoparticles (approximately 20–30 nm in diameter) increased with increasing electrodeposition times. The surface of the electrode clearly showed that the Pt nanoparticles homogeneously and uniformly gathered to fill the space on the surface of the Ti mesh, and the Ti mesh could completely filled after electrodeposition times of 400 s. Fig. 5d shows the cyclic voltammogram for the three Pt/Ti counter electrodes, and these Pt/Ti counter electrodes show two pairs of oxidation and reduction peaks. The oxidation and reduction peaks on the left (peaks *A*<sub>ox</sub> and *A*<sub>red</sub>) result from the redox reaction of 3I<sub>2</sub> + 2e<sup>-</sup> → 2I<sub>3</sub><sup>-</sup>, which has little effect on the DSSC performance; in contrast, the redox pair on the right (peaks *B*<sub>ox</sub> and *B*<sub>red</sub>) is attributed to the reaction of I<sub>3</sub><sup>-</sup> + 2e<sup>-</sup> → 3I<sup>-</sup>, which directly affects the DSSC performance [30,31]. The Pt/Ti counter electrode with an electrodeposition time of 400 s showed the largest oxidation and reduction current density, likely because this electrode contained the largest number of Pt nanoparticles on

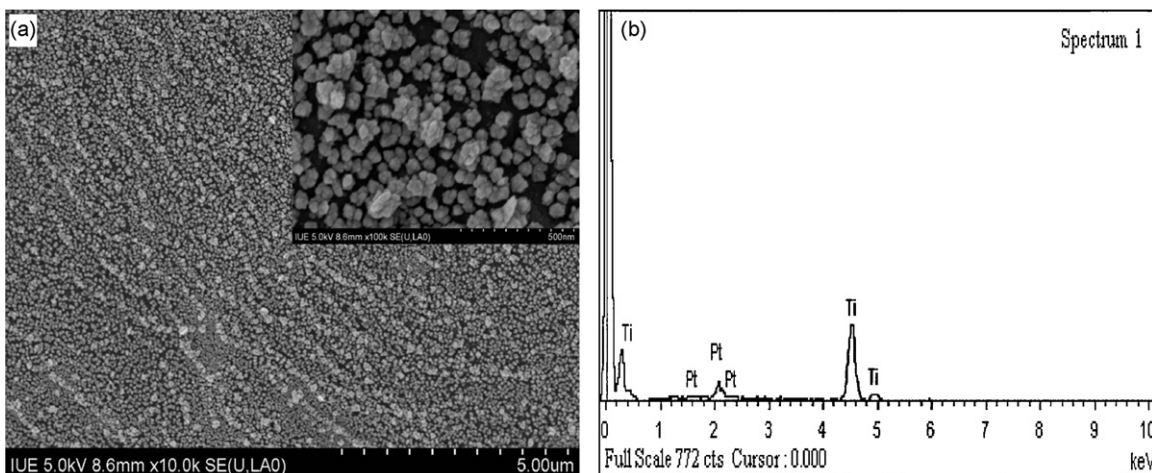


Fig. 4. SEM image (a) and EDS (b) of the Pt/Ti counter electrode.

the surface of the Ti mesh. From the SEM images in Fig. 5c and d, it appears that the optimal electrodeposition time to fabricate Pt/Ti counter electrodes is 400 s.

### 3.3. Models of Ti mesh

Electrochemical impedance spectroscopy (EIS) for the Pt/Ti electrodes with the same area of  $80 \text{ cm}^2$  and the different models (TB  $\times$  TL:  $1.0 \text{ mm} \times 2.0 \text{ mm}$ ,  $1.5 \text{ mm} \times 2.0 \text{ mm}$ ,  $1.5 \text{ mm} \times 2.5 \text{ mm}$

and  $1.8 \text{ mm} \times 2.5 \text{ mm}$ , respectively) was measured and shown in Fig. 6. Based on the EIS, the values of  $R_S$  and  $R_{CT}$  were obtained and shown in the table accompanying Fig. 6, where TB is the diagonal line breadth of the Ti mesh, TL is the diagonal line length of the Ti mesh,  $R_S$  is the series resistance of the Pt/Ti electrode, and  $R_{CT}$  is the charge-transfer resistance on the electrolyte|electrode interface for the  $\text{I}_3^-/\text{I}^-$  redox reaction [31,32]. It can be seen that the  $R_S$  increases with the increase of TB and TL. The  $R_S$  values increase from  $50.50 \Omega \text{ cm}^2$  for the mesh unit area  $1.00 \text{ mm}^2$  to  $56.34 \Omega \text{ cm}^2$

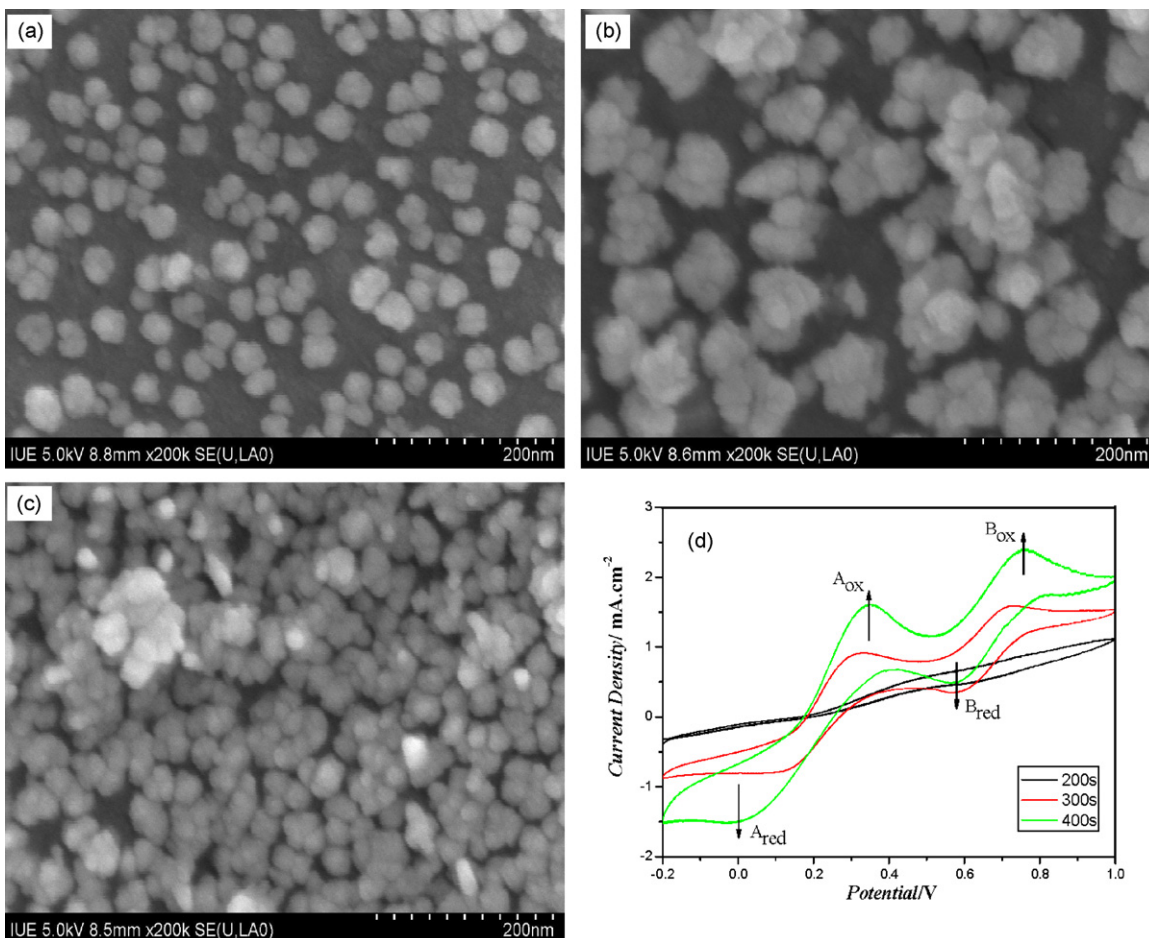
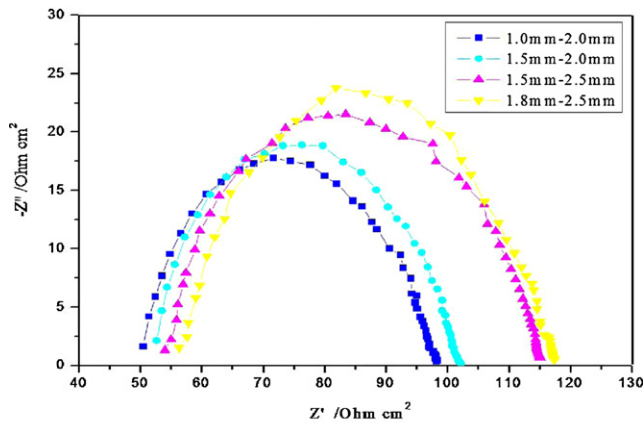


Fig. 5. SEM images of Pt/Ti electrode electrodeposited times of 200 s (a), 300 s (b) and 400 s (c), and their CV curves (d).

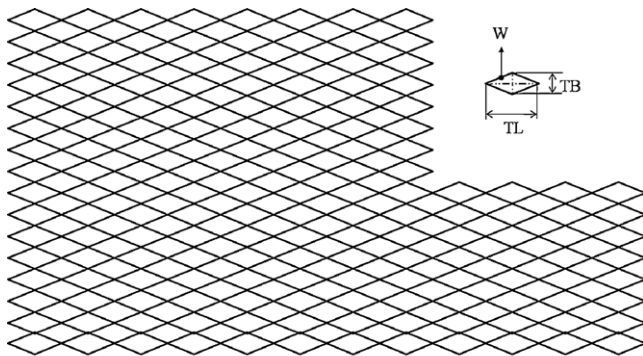


Model	$R_s (\Omega\text{-cm}^2)$	$R_{CT} (\Omega\text{-cm}^2)$
1.0mm-2.0mm	$50.50 \pm 0.03$	$47.68 \pm 0.04$
1.5mm-2.0mm	$52.63 \pm 0.05$	$49.57 \pm 0.04$
1.5mm-2.5mm	$53.99 \pm 0.02$	$61.08 \pm 0.03$
1.8mm-2.5mm	$56.34 \pm 0.04$	$61.15 \pm 0.05$

Fig. 6. EIS of Pt/Ti electrodes with different Ti mesh models.

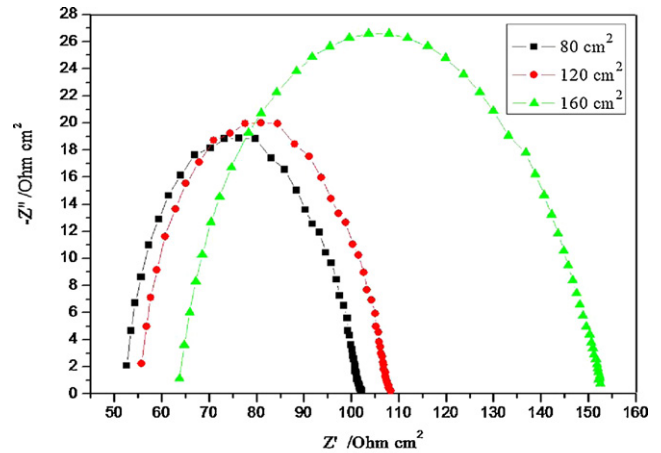
for the mesh unit area  $2.25 \text{ mm}^2$ , indicating the Pt/Ti electrode with the smaller mesh has a higher electrical conductivity that is favorable to electron transport [33–36]. The  $R_{CT}$  values also increase with the mesh unit area increase. Moreover the increase extent is larger than the  $R_s$ . The  $R_{CT}$  values increase from  $47.68 \Omega \text{ cm}^2$  for the mesh unit area  $1.00 \text{ mm}^2$  to  $61.15 \Omega \text{ cm}^2$  for the mesh unit area  $2.25 \text{ mm}^2$ , demonstrating that the Ti mesh model, especially in TL (the diagonal line length), could significantly influence the charge-transfer resistance on the electrolyte|electrode interface for the  $\text{I}_3^-/\text{I}^-$  redox reaction.

Fig. 7 shows the structure diagram of the Ti mesh and the computational formula of the Ti mesh light transmittance. Here, TB is the diagonal line breadth, TL is the diagonal line length of the Ti mesh, and W is the width of the Ti mesh infarction. The light transmittances of the Ti mesh were calculated using a computational formula and are summarized in Table 1. As shown in Table 1, the light transmittance of the Ti mesh increases with increasing values of TB and TL.



$$\text{Light transmittance}(\%) = \frac{\frac{1}{2}TB \times TL}{\frac{1}{2}TB \times TL + 4 \times (\frac{1}{2}W) \times \sqrt{(\frac{1}{2}TB)^2 + (\frac{1}{2}TL)^2}} \times 100\%$$

Fig. 7. Structure diagram of the Ti mesh and the computational formula of the Ti mesh light transmittance.



Size	$R_s (\Omega\text{-cm}^2)$	$R_{CT} (\Omega\text{-cm}^2)$
$80 \text{ cm}^2$	$52.63 \pm 0.05$	$49.57 \pm 0.04$
$120 \text{ cm}^2$	$55.79 \pm 0.04$	$52.55 \pm 0.05$
$160 \text{ cm}^2$	$63.78 \pm 0.05$	$88.74 \pm 0.06$

Fig. 8. EIS of Pt/Ti electrodes with different Ti mesh areas.

The photovoltaic properties of flexible DSSCs with the same rectangular dimension,  $21 \text{ cm} \times 4.5 \text{ cm}$ , with different Ti mesh models were measured under an outdoors natural light irradiation with an intensity of  $55 \text{ mW cm}^{-2}$ . The active area of the flexible DSSC was  $20 \text{ cm} \times 4.0 \text{ cm}$ , and the results are summarized in Table 1. These DSSCs have comparatively similar  $V_{OC}$  ( $0.725 \text{ V}$ ) values, because the  $V_{OC}$  is mainly determined by the energy level difference between the Fermi level of the electrons in  $\text{TiO}_2$  and the redox potential of the electrolyte [1,2]. Because these flexible DSSCs have the same compositions, their  $V_{OC}$  values are similar. As shown, the  $I_{SC}$  values increase with increasing values of TB and TL; this result occurs because the light transmittances of Ti mesh increase as the size of the mesh increases. However, the fill factor (FF) values are reduced as the size of the mesh increases, because the values of  $R_s$  and  $R_{CT}$  of the large-area ( $80 \text{ cm}^2$ ) flexible DSSCs are enlarged with the increase of the values of TB and TL [19,22,23]. Therefore, the  $\eta$  and  $P_{max}$  values of the DSSC first increase and then decrease as the size of the Ti mesh increases. Considering the light transmittance,  $R_s$  and  $R_{CT}$ , we choose the  $1.5 \text{ mm} \times 2.0 \text{ mm}$  model, whose the light transmittance is  $92.31\%$  and whose  $R_s$  and  $R_{CT}$  values are  $52.63 \pm 0.05 \Omega \text{ cm}^2$  and  $49.57 \pm 0.04 \Omega \text{ cm}^2$ , respectively.

### 3.4. Large-area flexible DSSCs

Electrochemical impedance spectroscopy (EIS) for the Pt/Ti electrodes in the same model of  $1.5 \text{ mm} \times 2.0 \text{ mm}$  and the different area were measured and shown in Fig. 8. These electrodes' rectangular areas included:  $21 \text{ cm} \times 4.5 \text{ cm}$ ,  $21 \text{ cm} \times 6.5 \text{ cm}$  and  $21 \text{ cm} \times 8.5 \text{ cm}$ , with active areas  $20 \text{ cm} \times 4.0 \text{ cm}$ ,  $20 \text{ cm} \times 6.0 \text{ cm}$  and  $20 \text{ cm} \times 8.0 \text{ cm}$ , respectively. According to the EIS, the  $R_s$  and  $R_{CT}$  values are calculated and shown in the table accompanying Fig. 8. The values of  $R_s$  and  $R_{CT}$  increase with the increase of Pt/Ti electrode areas, implying that the larger area Pt/Ti electrodes have a lower electrical conductivity, which is disadvantageous to electron transport [33–36]. However, the growth rate of the  $R_s$  and  $R_{CT}$  values with area is obviously less than that of other large-area flexible electrodes, suggesting that the Ti mesh is suitable for the large-scale preparation of Pt/Ti counter electrodes and flexible DSSCs.

**Table 1**  
The photovoltaic performance of flexible DSSCs with different Ti mesh models.

TB (mm)	TL (mm)	W (mm)	Light transmittance (%)	$I_{sc}$ (A)	$V_{oc}$ (V)	FF	$\eta$ (%)	$P_{max}^a$ (W)
1.0	2.0	0.05	89.94	0.486	0.725	0.717	5.74	0.253
1.5	2.0	0.05	92.31	0.518	0.729	0.714	6.13	0.270
1.5	2.5	0.05	92.79	0.520	0.726	0.705	6.05	0.266
1.8	2.5	0.05	93.59	0.525	0.728	0.684	5.94	0.261

$$^a P_{max} = I_{sc} \times V_{oc} \times FF.$$

**Table 2**  
The photovoltaic performance of the flexible DSSCs with different areas.

Size (cm <sup>2</sup> )	Solar intensity (mW cm <sup>-2</sup> )	$I_{sc}$ (A)	$J_{sc}$ (mA cm <sup>-2</sup> )	$V_{oc}$ (V)	FF	$\eta$ (%)	$P_{max}$ (W)
80	55	0.518	6.48	0.729	0.714	6.13	0.270
120	55	0.770	6.42	0.722	0.703	5.92	0.391
160	55	0.930	5.81	0.711	0.670	5.23	0.443

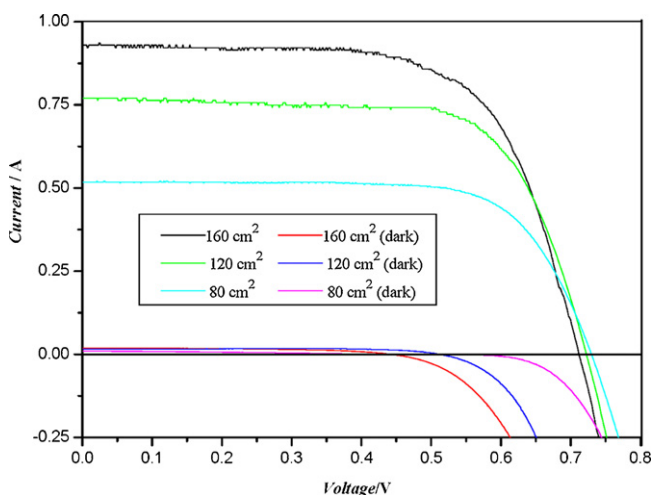


**Fig. 9.**  $I$ - $V$  curves of the flexible DSSCs with different areas (under an outdoors natural light irradiation with intensity of 55 mW cm<sup>-2</sup> and in the dark).

Fig. 9 shows the  $I$ - $V$  curves of the flexible DSSCs with Pt/Ti counter electrodes in the same model of 1.5 mm  $\times$  2.0 mm and different areas under an outdoors natural light irradiation with an intensity of 55 mW cm<sup>-2</sup> and in the dark. The photovoltaic performance of the flexible DSSCs are summarised in Table 2. It can be seen that with the decrease of the area of the flexible DSSC, the values of  $J_{sc}$ ,  $V_{oc}$  and FF increase, thus, the light-to-electric conversion efficiency ( $\eta$ ) increase, which is due to that the values of  $R_s$  and  $R_{CT}$  increase with the increase of the area of flexible Pt/Ti mesh electrodes [19,22,23]. When the area of the flexible DSSC is 80 cm<sup>2</sup>, the efficiency reaches 6.13%. The efficiency could be enhanced further if the flexible DSSC area is reduced or a new design is adopted. On the other hand, the photocurrent ( $I$ ) and maximum power output ( $P_{max}$ ) of the flexible DSSC increases with the increase of its area, which is due to that the  $P_{max}$  enhancement via increasing area exceeds to the expense by  $R_s$  and  $R_{CT}$ . When the area of the flexible DSSC is 160 cm<sup>2</sup>, the power output reaches 0.443 W. If the area of the flexible DSSC is enlarged or a new design is adopted, the power output could be enhanced further.

#### 4. Conclusion

In summary, titanium mesh was used to fabricate a Pt/Ti counter electrode by a chronoamperometry method. The optimal electrodeposition time to fabricate Pt/Ti counter electrodes on the Ti mesh in these systems was 400 s. The Pt/Ti counter electrode showed a relatively good light transmittance of 92.31%, a high electrocatalytic activity for the  $I_3^-/I^-$  redox reaction, a low series

resistance of  $52.63 \pm 0.05 \Omega \text{ cm}^2$  and a charge-transfer resistance of  $49.57 \pm 0.04 \Omega \text{ cm}^2$  with an area of 80 cm<sup>2</sup>. Based on the counter electrode, a light-to-electric energy conversion efficiency of 6.13% is achieved for a flexible DSSC with an area of 80 cm<sup>2</sup>, and a maximum power output of 0.443 W is reached for a flexible DSSC with an area of 160 cm<sup>2</sup>, under an outdoors natural light irradiation with an intensity of 55 mW cm<sup>-2</sup>. Compared with other materials used to prepare Pt counter electrodes, the Ti mesh has a relatively low sheet resistance and superior corrosion resistance for the electrolyte contacting  $I^-/I_3^-$ ; therefore, it is suitable for the large-scale preparation of flexible Pt/Ti counter electrodes. The present findings should accelerate the practical application of flexible DSSCs.

#### Acknowledgments

The authors would like to thank the joint support of the National High Technology Research and Development Program of China (No. 2009AA03Z217) and the National Natural Science Foundation of China (No. 90922028, 51002053).

#### References

- [1] B. O' Regan, M. Grätzel, *Nature* 353 (1991) 737.
- [2] M. Grätzel, *Inorg. Chem.* 44 (2005) 6841.
- [3] M. Grätzel, *Acc. Chem. Res.* 42 (2009) 1788.
- [4] F.C. Krebs, T. Tromholt, M. Jorgensen, *Nanoscale* 2 (2010) 873.
- [5] F.C. Krebs, T.D. Nielsen, J. Fyenbo, M. Wadstrom, M.S. Pedersen, *Energy Environ. Sci.* 3 (2010) 512.
- [6] M. Manceau, D. Angmo, M. Jorgensen, F.C. Krebs, *Org. Electron.* 12 (2011) 566.
- [7] F.C. Krebs, J. Fyenbo, D.M. Tanenbaum, S.A. Gevorgyan, R. Andriessen, B. Remoortere, Y. Galagan, M. Jorgensen, *Energy Environ. Sci.* (2011), doi:10.1039/c1ee01891d.
- [8] M. Grätzel, *Nature* 414 (2001) 338.
- [9] A. Hagfeldt, G. Boschloo, L. Sun, L. Kloo, H. Pettersson, *Chem. Rev.* 110 (2010) 6595.
- [10] Y.M. Xiao, J.H. Wu, G.T. Yue, G.X. Xie, J.M. Lin, M.L. Huang, *Electrochim. Acta* 55 (2010) 4573.
- [11] H.W. Chen, K.C. Huang, C.Y. Hsu, C.Y. Lin, J.G. Chen, C.P. Lee, L.Y. Lin, R. Vittal, K.C. Ho, *Electrochim. Acta* 56 (2010) 7991.
- [12] Y.M. Xiao, J.H. Wu, G.T. Yue, J.M. Lin, M.L. Huang, Z. Lan, *Electrochim. Acta* 56 (2011) 8545.
- [13] V. Vijayakumar, A.D. Pasquier, D.P. Birnie III, *Sol. Energy Mater. Sol. Cells* 95 (2011) 2120.
- [14] M. Ikegami, K. Miyoshi, T. Miyasak, *Appl. Phys. Lett.* 90 (2007) 153122.
- [15] S. Ito, N.C. Ha, G. Rothenberger, P. Liska, P. Comte, S.M. Zakeeruddin, P. Péchy, M.K. Nazeeruddin, M. Grätzel, *Chem. Commun.* 38 (2006) 4004.
- [16] M.D. Thomas, R.U. Patrick, R.W. Neil, V.M. Julie, *J. Am. Chem. Soc.* 127 (2005) 10639.
- [17] M.G. Kang, N.G. Park, K.S. Ryu, S.H. Changa, K. Kim, *Sol. Energy Mater. Sol. Cells* 90 (2006) 574.
- [18] J.H. Park, Y. Jun, H.G. Yun, S.Y. Lee, M.G. Kang, *J. Electrochem. Soc.* 155 (2008) F145.
- [19] K. Okada, H. Matsui, T. Kawashima, T. Ezure, N. Tanabe, *J. Photochem. Photobiol. A* 164 (2004) 193.
- [20] M. Biancardo, K. West, F.C. Krebs, *Sol. Energy Mater. Sol. Cells* 90 (2006) 2575.
- [21] G.R.A. Kumara, S. Kaneko, A. Konno, M. Okuya, K. Murakami, B. Onwona-ogyeman, K. Tennakone, *Prog. Photovoltaics: Res. Appl.* 14 (2006) 643.

- [22] W.J. Lee, E. Ramasamy, D.Y. Lee, J.S. Song, *J. Photochem. Photobiol. A* 183 (2006) 133.
- [23] E. Ramasamy, W.J. Lee, D.Y. Lee, J.S. Song, *J. Power Sources* 165 (2007) 446.
- [24] S. Noda, K. Nagano, E. Inoue, T. Egi, T. Nakashima, N. Imawaka, M. Kanayama, S. Iwata, K. Tushima, K. Nakada, K. Yoshino, *Synth. Met.* 159 (2009) 2355.
- [25] D.H. Yeon, K.K. Kim, N.G. Park, Y.S. Cho, *J. Am. Ceram. Soc.* 93 (6) (2010) 1554.
- [26] J.H. Wu, Z. Lan, J.M. Lin, M.L. Huang, S.C. Hao, T. Sato, S. Yin, *Adv. Mater.* 19 (2007) 4006.
- [27] J.H. Wu, S.C. Hao, Z. Lan, J.M. Lin, M.L. Huang, Y.F. Huang, P.J. Li, S. Yin, T. Sato, *J. Am. Chem. Soc.* 130 (2008) 11568.
- [28] Z. Lan, J.H. Wu, S.C. Hao, J.M. Lin, M.L. Huang, Y.F. Huang, *Energy Environ. Sci.* 2 (2009) 524.
- [29] M. Grätzel, *Prog. Photovoltaics: Res. Appl.* 8 (2000) 171.
- [30] Z. Huang, X.Z. Liu, K.X. Li, D.M. Li, Y.H. Luo, H. Li, W.B. Song, L.Q. Chen, Q.B. Meng, *Electrochem. Commun.* 9 (2007) 596.
- [31] X. Mei, S. Cho, B. Fan, J.Y. Ouyang, *Nanotechnology* 21 (2010) 395202.
- [32] G. Li, F. Wang, Q. Jiang, X. Gao, P. Shen, *Angew. Chem. Int. Ed.* 49 (2010) 3653.
- [33] A. Fujiwara, Y. Matsuoka, Y. Matsuoka, H. Suematsu, N. Ogawa, K. Miyano, H. Kataura, Y. Maniwa, S. Suzuki, Y. Achiba, *Carbon* 42 (2004) 919.
- [34] S. Moriyama, K. Toratani, D. Tsuya, M. Suzuki, Y. Aoyagi, K. Ishibashi, *Physica E* 24 (2004) 46.
- [35] G. Mor, K. Shankar, M. Paulose, O. Varghese, C. Grimes, *Nano Lett.* 6 (2006) 215.
- [36] H. Lin, N. Wang, L. Zhang, *Adv. Technol. Mater. Mater. Process. J.* 9 (2007) 5.